NUMERICAL AND EXPERIMENTAL STUDIES ON PRODUCTION OF FINE SILICA IN AN OPPOSED FLUIDIZED BED AIR JET MILL

by

SRI RAJ RAJESWARI A/P MUNUSAMY

Thesis submitted in fulfillment of the requirements for the degree of Doctor of Philosophy

November 2011

ACKNOWLEDGEMENTS

My greatest debt of gratitude to Almighty GOD, for his grace which enables me to complete my research studies. I would like to express my greatest debt of inadequate acknowledgement to Professor Dr. Khairun Azizi Bt. Mohd. Azizli, Professor Dr. Mohd. Zulkifly Abdullah and Dr. Syed Fuad Saiyid Hashim for their encouragement, prestigious guidance, helpful suggestions and consistent supervisions throughout this research work.

My greatest appreciation is also extended to Universiti Sains Malaysia, Institute of Postgraduate Studies and School of Materials and Mineral Resources Engineering for providing me with USM Fellowship Scholarship to conduct and complete my studies. I am also thankful to Dean, Deputy Dean, lecturers and all technical staffs at School of Materials and Mineral Resources Engineering, School of Mechanical Engineering and School of Aerospace Engineering for all the assistance, support and guidance throughout my research studies. My appreciation also goes to Universiti Teknologi Petronas and the staffs there for helping and providing me with all the necessary facilities to complete my Ph.D thesis successfully.

My greatest gratitude and appreciation is also extended to my father, Mr. T. Munusamy, mother, Mrs. M. Sarasvathy, brother Mr. M. Shanmugaveloo and sisters M. Parameswari and M. Retna Devi for their continuos support and encouragement till today. Last but not least, I would like to thank all my friends for their help throughout my studies.

SRI RAJ RAJESWARI A/P MUNUSAMY

TABLE OF CONTENTS

CHAPTER 3 : METHODOLOGY

LIST OF TABLES

LIST OF FIGURES

LIST OF ABBREVIATIONS

3-D	Three-dimensional
2-D	Two-dimensional
BJH	Baret-Joyner-Halenda
DEM	Discrete Element Method
BET	Brunauer, Emmet and Teller
CAD	Computer Aided Design
CFD	Computational Fluid Dynamics
CS or N	Classifier rotational speed
CTE	Coefficient of Thermal Expansion
DOC	Degree of crystallinity
EGM	Eulerian Granular Model
FP	Feed pressure
FEM	Finite Element Method
FDM	Finite Difference Method
FVM	Finite Volume Method
FWHM	Full width at half maximum
GP or P	Grinding Pressure
hkl	Diffraction plane
ICDD	International Center for Diffraction Data
IUPAC	International Union of Pure and Applied Chemistry
KTGF	Kinetic Theory of Granular Flow
rpm	Revolutions per minute
SEM	Scanning Electron Microscope
SIMPLEC	Semi-Implicit Method for Pressure-Linked Equations
SFR	Solid Feed Rate
SSA	Specific surface area
SD	Separation Distance
XRD	X-ray Diffraction

LIST OF SYMBOLS

$\dot{m}_T$	Mixture mass flow rate, kg/s
$\dot{m}_s$	Solid mass flow rate, kg/s
$\dot{m}_g$	Air mass flow rate, kg/s
$\dot{m}_{pq}$	Mass transfer from phase *p* to phase *q*
$\dot{m}_{qp}$	Mass transfer from phase *q* to phase *p*
τ_s	Particulate relaxation time
Q	Volumetric air flow rate, m^3/h
V_g	Air velocity, m/s
V_s	Solid velocity, m/s
d_s	The diameter of the s^{th} solid phase particles, µm
d_i	Initial mean diameter, µm
d_f	Final mean diameter, µm
d(4.3)	Volume moment diameter, µm
d_{50}	Mean diameter of solid, µm
d_{90}	90% passing size of solid, µm
d(v,0.5)	50% passing size of solid, µm
d (v,0.9)	90% passing size of solid, µm
d (v,0.1)	10% passing size of solid, µm
d_t	Classifier's cut point, µm
x_c	Cut size of particle, µm
x_k	Number percentage of detected diameter
d_k	Detected diameter
I_{2D}	Second invariant of the deviatoric stress tensor
$\bar{\bar{I}}$	Identity tensor
C_D	Drag coefficient
$\mathrm{Re_s}$	Relative Reynolds number between phase's g and s
$g_{O,ss}$	Radial distribution function
e_{ss}	Coefficient of restitution for particle collisions
$\vec{v}_q$	Velocity of phase *q*, m/s
$\vec{v}_s$	Velocity of solid phase, m/s
$\vec{v}_g$	Velocity of air phase, m/s
$\vec{v}_q^T$	Indicates the transpose, m/s
$\vec{v}_{pq}$	Interphase velocity
$v_{r,s}$	Terminal velocity correction for the solid phase, m/s
$\vec{g}$	Gravity acceleration, m/s^2
$K_{pq} = K_{qp}$	Interphase momentum exchange coefficient
K_{sl}	Fluid-solid exchange coefficient

K_{sg}	Interphase momentum exchange coefficient for gas-solid
K_{gs}	Interphase momentum exchange coefficient for solid-gas
p	Pressure shared by all phases
P_s	Total solid pressure
$\vec{F}_q$	External body force
$\vec{F}_{lift,q}$	Lift force for phase q
$\vec{F}_{vm,q}$	Virtual mass force for phase q
$\vec{F}_{ex,s}$	External body force for solid
$\vec{F}_{lift,s}$	Lift force for solid
$\vec{F}_{vm,s}$	Virtual mass force for solid
$\vec{R}_{pq}$	Interaction force between phases
$\mathrm{M_{JMEXPFEED}}$	Experimental jet mill feed mass, kg
$\mathrm{M_{CYCEXPFEED}}$	Experimental cyclone feed mass, kg
$\mathrm{M_{GC}}$	Mass retained in the grinding chamber, kg
$\mathrm{M_{CYCEXPU/F}}$	Experimental cyclone underflow mass, kg
$\mathrm{M_{CYCEXPO/F}}$	Experimental cyclone overflow mass, kg
R_{gr}	Grinding rate
Rj	Rupture of joints
Ch	Chipping
Cl	Cleavage
Gr	Ultimate grinding
S_q	Source term
W_m	Monolayer adsorbed gas quantity
M_s	Mass of silica exiting the air jet mill's pressure outlet boundary, kg
D_v	Volume weighted mean of the crystallite size
Am	amorphization
A_o	Area under the peak for feed
A_t	Area under the peak for ground products
d_N	Nozzle exit diameters
N1, N2, N3	Grinding nozzles
w	Pore width, nm
t	Time, s
K	constant
$\mathrm{P_{in}}$	Pressure inlet, bars
$\mathrm{P_{out}}$	Pressure outlet, bars
F_g	Gravitational force
F_c	Centrifugal force
Q_{EVS}	Equisize Skew

Q_{EAS}	Equiangle Skew
Q_{AR}	Aspect ratio

Greek Symbols

α_q	Phase volume fraction
α_s	Volume fraction of solid
α_g	Volume fraction of gas
$\alpha_{s,max}$	Maximum value for solid volume fraction
$\bar{\alpha}_s$	Average solid volume fraction
α_d	Volume fraction of dispersed phase
α_c	Volume fraction of carrier phase
α_p	Volume fraction of particle
$\bar{\alpha}_g$	Average air volume fraction
ρ_s	Solid density, kg/m^3
ρ_g	Gas density, kg/m^3
μ_q	Shear viscosity of phase q, kg/m.s
μ_s	Solids shear viscosity, kg/m.s
$\mu_{s,col}$	Collisional part of shear viscosity, kg/m.s
$\mu_{s,kin}$	Kinetic part of shear viscosity, kg/m.s
$\mu_{s,fric}$	Frictional part of shear viscosity, kg/m.s
μ_g	Shear viscosity for gas, kg/m.s
$\bar{\bar{\tau}}_q$	Phase stress-strain tensor, Pa
$\bar{\bar{\tau}}_s$	Stress-strain tensor for solid, Pa
$\bar{\bar{\tau}}_g$	Stress-strain tensor for gas, Pa
λ_q	Bulk viscosity for phase q, kg/m.s
λ_s	Bulk viscosity for solid phase, kg/m.s
θ_s	Granular temperature, m^2/s^2
ϕ	Frictional angle
π	Pi
γ	Material density ratio
ρ_d	Density of dispersed phase
ρ_c	Density of carrier phase
$\hat{\rho}_q$	Effective density of phase q
β	Particulate loading
θ	Bragg angle of hkl reflection
λ	Wavelength
ε	Lattice strain
ψ	Span value

KAJIAN BERANGKA DAN EKSPERIMEN KE ATAS PENGHASILAN SILIKA HALUS DI DALAM PENGISAR JET UDARA LAPISAN TERBENDALIR BERTENTANGAN

ABSTRAK

Penyelidikan ini adalah tertumpu ke atas penghasilan silika halus di dalam pengisar jet udara lapisan terbendalir bertentangan melalui teknik berangka dan eksperimen. Pengisaran halus di dalam pengisar jet udara berlaku melalui perlanggaran di antara partikel pepejal di dalam arus udara yang berterusan. Peringkat yang terlibat di dalam teknik berangka termasuklah pemodelan tiga dimensi (3-D) dan simulasi pengisar jet udara dengan menggunakan perisian GAMBIT 2.3.16 dan FLUENT 6.3. Sejumlah 144,237 unsur jaringan T-Grid dan 422 unsur jaringan Pave hadir di bahagian domain utama pengisar jet udara dan bahagian muncungnya. Pemodelan aliran udara-pepejal di dalam pengisar jet udara adalah berasaskan kaedah model partikel Eulerian (EGM) dengan model gelora k-epsilon serta fungsi seretan Syamlal-O'Brien. Jisim keluaran silika daripada pengisar jet udara digunakan untuk menentusahkan model CFD dengan eksperimen. Perbezaan jisim keluaran di antara 11.50% dan 19.97% menunjukkan model adalah sesuai dan memuaskan untuk simulasi proses pengisaran halus. Perubahan di dalam parameter pengoperasian pengisar jet udara mempengaruhi aliran udara dan pepejal serta ciri-ciri produk terkisar. Halaju angin dan pepejal, V_g dan V_s tertabur di antara 357.88 m/s dan 509.86 m/s serta 41.45 m/s dan 57.82 m/s manakala pecahan isipadu pepejal, $\bar{\alpha}_s$ di salur keluar pengisar jet udara adalah di antara 0.01 dan 0.03.

Pemerhatian menunjukkan pecahan isipadu pepejal adalah tinggi di bahagian tengah dan jauh dari bahagian muncung masing-masing. Pada kadar suapan pepejal dan tekanan pengisaran yang rendah, produk mengalami pengurangan saiz dengan garis pusat momen isipadu, $d(4.3)$ sehingga 8.66 µm. Keadaan ini disebabkan oleh perlanggaran berkesan partikel apabila pecahan isipadu pepejal, α_s dan halaju fasa, V_g dan V_s adalah rendah. Produk bagi kadar suapan pepejal yang tinggi mempunyai luas permukaan tentu terendah bernilai 3.066 m^2/g disebabkan penetrasi jet udara dan aktiviti perlanggaran di antara partikel pepejal di dalam arus udara yang tidak efektif pada bebanan partikel yang tinggi. Peningkatan jumlah berliang meso (2-50 nm) dan mikro (< 2 nm) menunjukkan produk mempunyai taburan liang permukaan yang lebih luas berbanding silika suapan. Kristal bersaiz kasar dihasilkan pada tekanan pengisaran tinggi disebabkan oleh gelora, halaju fasa dan daya seretan tinggi yang menarik partikel pepejal lebih awal daripada kebuk pengisaran. Secara keseluruhannya, saiz kristal dan struktur terikan bagi produk adalah berjulat di antara 190 nm dan 453.5 nm serta 0.116 dan 0.187 manakala darjah pengkristalan adalah di antara 99.37% ke 76.57% berbanding dengan 100% bagi silika suapan.

NUMERICAL AND EXPERIMENTAL STUDIES ON PRODUCTION OF FINE SILICA IN AN OPPOSED FLUIDIZED BED AIR JET MILL

ABSTRACT

This study is mainly focused on the production of fine silica in an opposed fluidized bed air jet mill through numerical and experimental techniques. In this mill, fine grinding occurs through collisions between solid particles in the continuous air stream. The stages in numerical techniques include the three-dimensional (3-D) modeling and simulations of the air jet mill using GAMBIT 2.3.16 and FLUENT 6.3 softwares. The major domain of the air jet mill and the nozzle parts consist of 144,237 elements of T-Grid mesh and 422 elements of Pave mesh respectively. The Eulerian Granular Model (EGM) approach with k-epsilon turbulence model and Syamlal-O'Brien drag function was adopted for modeling the air-solid flows in air jet mill. Validations of the CFD model with experimental and numerical results were made based on the mass output of silica from the jet mill. The mass difference within 11.50% to 19.97% indicates that the model is fairly suitable and satisfactory for simulations of fine grinding process. Variations in the operating variables of air jet mill influence the air-solid flow fields and the product characteristics. The air and solid velocities, V_g and V_s vary from 357.88 m/s to 509.86 m/s and 41.45 m/s to 57.82 m/s respectively, while the solid volume fractions, $\bar{\alpha}_s$ at the air jet mill's pressure outlet are within 0.01 to 0.03.

Observations showed high solid volume fractions at the center and regions away from the nozzles. At low solid feed rate and grinding pressure, the products undergo size reduction with volume moment diameter, $d(4.3)$ up to 8.66 µm due to

effective particle collisions at lower solid volume fractions, α_s and phase velocities, V_g and V_s. The products of high solid feed rate have lowest specific surface area of 3.066 m^2/g due to ineffective penetration of air jets and collisional activities between the particles in the air stream at higher particulate loading. Increase in the amount of mesopores (2-50 nm) and micropores (< 2 nm) showed that the products have wider surface pore size distributions compared to feed silica. At high grinding pressure, coarser size crystallites are produced due to higher turbulence, phase velocities and drag force pulling the particles sooner from the grinding chamber. Overall, the crystallite size and lattice strains of products ranged between 190 nm to 453.5 nm and 0.116 to 0.187 while the degree of crystallinity varies from 99.37% to 76.57% compared to 100% in feed silica.

CHAPTER 1

INTRODUCTION

1.1 Fine Grinding

Classification of grinding mills are normally based on the typical feed and product sizes, usage of different type of grinding mediums, breakage mechanism within the mill and the specific energy input requirements (Wang and Forssberg, 2007). Various types of grinding mills such as fluid energy mill, stirred bead mill, vibrating ball mill, autogenous mill, pin mill, ball mill, roller mill, ring ball mill, rod mill and hammer mill are available for fine grinding purpose. Among all the mills, fluid energy mills or better known as air jet mills differ from the other types as the size reduction in these mills involves collisions between the particles in high speed air jets whereas other mills use grinding mediums such as balls, beads, etc. for its grinding purpose.

In recent years, product quality criteria has become more and more stringent, leading to specifications like narrower particle size distributions and hence closer control of particle size. The requirement for submicron fine particles is increasing tremendously due to the increasing need for fine ceramics, plastic, mineral and metal powders which have the advantages such as large specific area and high activity of particle surface and so forth (Vegt de *et al.*, 2009). Ultrafine grinding using jet mills seems to be the most versatile technique for obtaining ultrafine products with average particle sizes between 1 μm and 10 μm. It is widely used in various

industries such as minerals, chemicals, pharmaceuticals, pigments, papers, polymers, toners, ceramics, foodstuffs, metal oxides and carbon nanotubes with micron size particles exhibiting narrow size distribution, absence of contamination and ability to grind heat sensitive materials (Alfano *et al*., 1996; Benz *et al*., 1996; Tuunila and Nyström, 1998; Tasirin and Geldart, 1999; Midoux *et al*., 1999; McMillan *et al*., 2007b, Baddour *et al*., 2009).

Historically, the work on air jet milling is largely focused on the analytical and experimental studies. Irrespective of jet mill types, a number of researchers studied the influence of mill design, its operational variables and the raw material characteristics on the grinding performance and breakage mechanism of particles. These include works by Alfano *et al.* (1996), Mebtoul *et al.* (1996), Müller *et al.* (1996), Tuunila and Nyström (1998), Midoux *et al.* (1999), Berthiaux *et al.* (1999), Berthiaux and Dodds (1999), Frances *et al.* (2001), Godet-Morand *et al.* (2002), Nakach *et al.* (2004), Choi *et al.* (2004), Fukunaka *et al.* (2006), Vegt de *et al.* (2006, 2009), Sikong *et al*. (2008), Ahmad *et al*. (2008) and Palaniandy *et al.* (2008a,b,c; 2009a,b). Such work focused on the properties of fine particles produced through air jet milling process and their ability in enhancing the properties of various industrial products. Amongst others, fine particle properties such as particle size, particle shape, surface texture and mechanochemistry effects such as changes in crystallite sizes, lattice strains, degree of crystallinity and amorphism rate upon subjection to air jet milling were extensively discussed by these investigators. Accordingly, the jet mill products which varied in particle size, shape, surface texture and crystallite properties were mixed, blended and tested in rubber, plastic, composites, polymers and underfill encapsulants. Through product testing, Suhaida *et al*. (2011) proved

that substitution of irregular shape ultrafine silica particles in rubber resulted in highest tensile strength, tensile modulus and hardness followed by the elongated and cubical shape particles. Moreover, better dispersion of irregular shaped ultra fine silica had improved the adhesion between the ultrafine silica and the natural rubber matrix.

The grindability of various types of materials which ranges in hardness, densities and structure have also been reported. These include from the softest material on Mohr's hardness scale i.e. talc up to hard and abrasive material like silica which has a hardness of 7. Sikong *et al*. (2008) investigated the effect of material characteristics such as feed sizes, mineral or material hardness, density and crystal structure of gypsum, barite, ilmenite, quartz and ferrosilicon on fine grinding in air jet mill. Their findings showed that heavy minerals such as barite and ilmenite have finer product sizes than lighter minerals like quarts due to higher particle-particle and particle-wall collision forces which lead to production of fine size products with narrow size distributions. However, high hardness of quartz also results in a larger median size diameter. On the other hand, breakage of gypsum and barite along their cleavage planes results in narrow size distribution whereas quartz, ilmenite and ferrosilicon exhibited wider size distributions and angular shapes due to shattering and chipping breakage mechanism.

Apart from this, Vegt de *et al.* (2006, 2009) studied the effects of defects on minerals such as impurities, flaws and crystal defects towards air jet milling process. Experimental analyses showed that material with a relatively low hardness results in largest breakage rate of particles. The probability of a particle with certain size to

break per unit time is defined as the particle breakage rate. Overall, the crystal's flaw size and density of flaws has an impact on the mechanical properties and subsequently on the fracture behavior of particles in a jet mill.

1.2 Flow Fields in Air Jet Mill

Air jet mill is a complex grinding mill which functions both as fine grinding and classification device. It is a static grinding mill which does not have any grinding media and operates using fluid energy in a different manner from the other mechanical grinding mills. Basically, it consists of a grinding chamber, internal built-in classifier and nozzles pointing downwards at an angle. It uses high velocity jets of gas to impart energy and cause intense inter particle collisions and this has been used successfully for milling of materials that are difficult to break or for producing very fine particles (Chamayou and Dodds, 2007; Bentham *et al*., 2004). The schematic view of the overall process in Alpine 100 AFG opposed type jet mill is given in Figure 1.1.

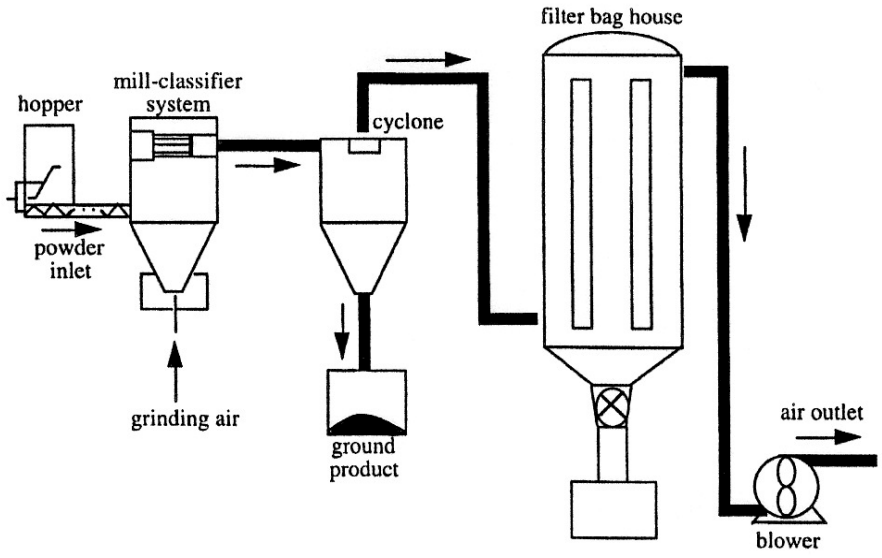

Figure 1.1: Schematic view of the overall process (Berthiaux and Dodds, 1999)

The flow fields in jet mill are complex owing to the multiphase interactions at various regimes of jet mill. Complexity in the flow fields within the jet mill is chiefly contributed by its sub-processes such as solid-gas interactions, collisions, motion of particles, turbulent flows, eddies, spiral vortices and 3-D complex swirling condition within the jet mill. Similar to other types of jet mills, the flow fields in opposed fluidized bed air jet mill is controlled by the mills design, its operational variables and material characteristics. However, this grinding device differentiates it from other types of grinding mills in terms of its design aspect and working principle. It houses the grinding nozzles which are used for grinding purposes at the bottom region of the jet mill whereas the feed enters from the top region of the mill. Inner portion of the mill is divided into grinding-classification region in which grinding occurs at the grinding region in the mill's grinding chamber while the dynamic classifier in the classification zone classifies the products leaving the jet mill.

Principally, air jet mill involves granular flow of gas-solid type with particle laden flow characteristics in which air represent the gas phase. It signifies the flow of discrete particles in a continuous air stream as illustrated in Figure 1.2.

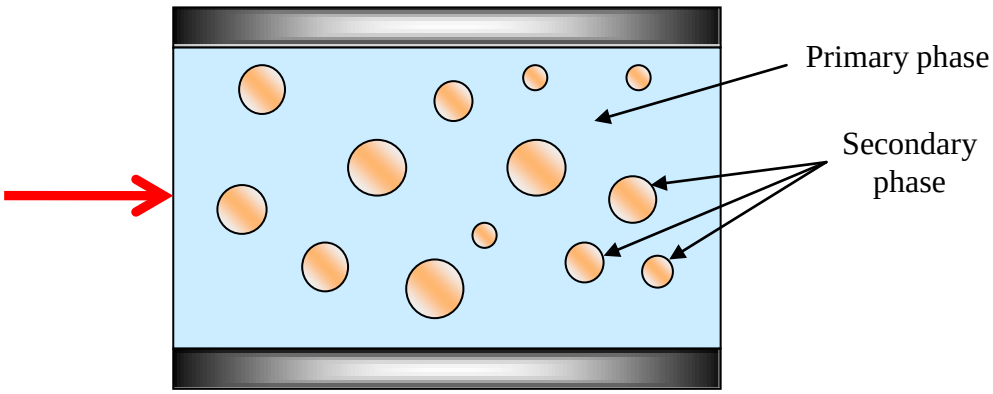

Figure 1.2: Primary continuous air phase and secondary solid phase dispersed in the primary phase (ANSYS Inc., 2006)

Obeying to the laws of conservation of mass and momentum (Newton's Second Law of Motion), phase volume fractions which signify the space occupied by the solid and air phases in a jet mill sums to one $\left(\sum_{q=1}^{n} \alpha_q = 1\right)$. As q represents the phases of the system, the total volume fraction for the air-solid flows in air jet mill system can be represented by Equation 1.1,

$$\alpha_s + \alpha_g = 1 \tag{1.1}$$

In which α_s and α_g represent the solid and air volume fractions respectively.

The phase interaction is associated with the particulate loading into the jet mill system. The particulate loading is defined as the mass density ratio of the dispersed phase (*d*) to that of the carrier phase (*c*) as given in Equation 1.2,

$$\beta = \frac{\alpha_d \rho_d}{\alpha_c \rho_c} \tag{1.2}$$

Where, α_d and α_c represent the volume fractions of dispersed and carrier phases while ρ_d and ρ_c are the density of dispersed and carrier phases respectively.

As stated by Baddour *et al.* (2009), the particle motion in the impact zone of jet mill is dependent on the particle inertia and the strength of the local gas eddies. Accordingly, as described in Fluent Inc. (2006), the interaction between the phases is one-way for very low loading in which the fluid carrier influences the particles via drag and turbulence. Meanwhile, two-way interactions occurs for intermediate loading in which the fluid carrier influences the particulate phase via drag and

turbulence but the particles in turn influence the carrier fluid via reduction in mean momentum and turbulence. Comparatively, for high loading there exist two-way interactions plus particle pressure and viscous stresses due to particles (four-way interactions). According to Hryb *et al*. (2008), one-way interactions occurs when the particle volume fraction, $\alpha^p < 10^{-6}$ while two-way interactions prevail when the $10^{-6} \leq \alpha^p \leq 10^{-3}$ whereas four-way interactions which designates dense particle concentrations occur when $\alpha^p > 10^{-3}$.

1.3 Factors Controlling Flow Fields in Air Jet Mill

The features of air-solid flows in jet mill are influenced by the mill's design, its operating variables and material characteristics. In view of design aspects, the nozzle properties such as its shape, size, angle, number, orientations and the separation distance between two opposing nozzles are of great importance in influencing the mill's grinding performance. Amongst the operating variables, solid feed rates, grinding air pressure and classifier speed play significant roles in grinding process although other variables such as type of grinding fluids was also mentioned by Zhao and Schurr (2002).

Higher air flow rate which is a function of the grinding pressure is capable in increasing the particle velocities, its collisional force and the velocity of the free spiral vortexes. Air jets are used to give high energy impacts between particles which are in suspension in fluidized bed opposed jet mills. As the gas kinetic energy is a square function of particle velocity $(E_k = \frac{1}{2} M_g {v_s}^2)$, acceleration of particles to the highest possible speeds is of critical importance. Therefore, the velocity of the

particle or its suspending fluid is of great importance as very low impact speeds results in no size reduction while too high impact speed leads towards over fines production. Accordingly, at higher gas and solid velocities, greater drag forces, F_D are induced to pull the particle sooner from the grinding zone. This is necessary in order to remove the ground products from the grinding zone apart from recirculating the coarse fractions into the grinding chamber for further grinding (Midoux *et al*., 1999; Tasirin and Geldart, 1999, Galk *et al*., 1999; Zhao and Schurr, 2002; Ma *et al*., 2001, Chamayou and Dodds, 2007, Sikong *et al*., 2008).

Conversely, increase in the particle concentrations reduces the distance travelled by the particles due to too many particle entrainments in the grinding chamber (Ma *et al*., 2001; Kolacz, 2004). In turn, the collisional velocity, the impact of collisions and breakage efficiency decelerates as the penetration of air jets into the particle decelerates. This results in low specific kinetic energy per particle and therefore low breakage probability. The velocity of free spiral vortexes reduce and particle with bigger size follows the vortex stream before leaving the mill at high particle concentrations. Hence, as mentioned by Kolacz (2004), an optimal mill filling level ensures best milling capacities and product stabilities as higher filling level results in damping of the material layer over the nozzle areas. Alternatively, low filling level generates turbulence, lower material layer over the nozzle area and damping effects which result in product instabilities.

In short, the design and operating variables affect the flow field of air-solid phases such as its concentrations, velocity, turbulence and the trajectories or motions within the mill during fine grinding process. These flow fields are important aspects

for an effective air-solid collisions, impacts and breakage. Therefore, fundamental understanding of the relationship between the mill design, operational variables, materials characteristics and air-solid flow fields will lead towards effective grinding, improved energy efficiency and better control of the ground product characteristics.

1.4 Problem Statement

Numerous studies have been accomplished on the effect of mills design, its operating variables and material characteristics towards the grinding performance of air jet mill. However, studies on the air-solid flow fields within air jet mill and its relationship with input variables, mills design and output product characteristics are still inadequate compared to other mineral processing devices such as cyclones. The motion of particles in a spiral jet mill was studied by Levy and Kalman (2007). Teng *et al.* (2009) investigated the flow field in the grinding chamber of Vortex type fluid energy mill by considering a three-dimensional turbulent model. Most recently, Teng *et al*. (2011) also focused on the particulate motions and collision inside the Vortex type fluid energy mill by coupling the Discrete Element Method (DEM) and Computational Fluid Dynamics (CFD) techniques. The influences of the operational conditions on the particulate motions and collisions were investigated and correlated with the size reduction process and types of breakage mechanism. Meanwhile, Liu and Chen (2009) developed a three-dimensional model of opposed superfine jet mill to investigate the internal flow fields. Despite of these few studies in particular on spiral type jet mills, numerical studies on the opposed fluidized bed air jet mill which is used for fine grinding purposes are still limited.

The air-solid flow fields such as the phase velocities and volume fractions are important factors controlling the particle collisions, breakage and fragmentation modes. Therefore, understanding the flow fields during fine grinding process in air jet mill and its effect on product qualities is of significant importance. High velocity collisional activities between particles in the carrier air stream results in high mill turbulence especially at the jetting region of air jet mill. As the mill design and material characteristics are kept consistent, variation in the air-solid flow fields and the mill turbulence are primarily influenced by the mill's operating variables such as its solid feed rate, grinding air pressure and classifier speeds. Consequently, the velocities and volume fractions of the air-solid phases within various regions of air jet mill changes with variation in the mill's operating variables. This in turn, influence the breakage rate, fragmentation modes, product characteristics as well as the amount of silica transported out of the jet mill's domain.

This work involves numerical and experimental studies of air jet mill. In this work, a CFD model of air jet mill will be developed to study and understand the flow fields of air-solid phases and its influence on the grinding process. The information on the dual phase volume fraction profiles, turbulence parameters such as dual phase velocity vectors, contours and path lines of phases which are hard to obtain in laboratory conditions are easily visualized by using CFD techniques without interfering the flow by internal probes. Apart from flow visualization, the types of interactions between the air-solid phases with changes in operating variables, design specifications and material characteristics during fine grinding process can be determined through CFD simulation approach. Following to this, the internal flow fields of air-solid phases can be interrelated with the resulting product characteristics.

This in turn can lead towards improvement of the mill performance for better control of product characteristics.

1.5 Objectives

The main objective of this research is to study the production of fine silica in an opposed fluidized bed air jet mill through numerical and experimental techniques. The measurable objectives are:-

- To develop a Computational Fluid Dynamics (CFD) model of air jet mill for numerical studies of fine grinding process using CFD modeling and simulation techniques.

- To verify the suitability and validity of the CFD model of air jet mill through numerical and experimental techniques by determining the mass of silica exiting the air jet mill's pressure outlet.

- To investigate the flow fields of air-solid phases in air jet mill with variations in the operational variables (grinding pressure, solid feed rate, classifier speed) at a fixed mill design and feed material characteristics using the CFD model.

- To study the product characteristics such as particle size, surface pore characteristics, specific surface areas, morphological properties (particle shape and its surface texture) and crystallite properties with changes in operating variables of the air jet mill experimentally.

- To determine the overall relationship between product characteristics with operating conditions of air jet mill and air-solid flow fields.

The results of this work are expected to provide valuable information and better understanding of fine grinding process in air jet mill particularly on the flow fields of its air-solid phases. The knowledge on the salient features of the mill and the type of interaction between the air-solid phases are of utmost importance. The flow fields and interactions between the air-solid phases are dependent on the mill's operating conditions as the mill design and material characteristics are consistent. Consequently, the changes in air-solid flow fields influence the product characteristics. This information can be used in the control and improvement of the fine grinding process which will lead to more efficient grinding process for production of high quality products for various applications.

1.6 Scope of work

The scope of this work includes numerical and experimental studies of fine grinding of silica in air jet mill. At a fixed machine design and material characteristics, the effect of changes in operating variables and air-solid flow fields on the product characteristics will be investigated in detail. The stages involved in the numerical and experimental studies are as follows:-

- Development of a three-dimensional (3-D) model of air jet mill using GAMBIT 2.3.16 CAD pre-processor.

- Validation of the air jet mill model for its suitability, accuracy and consistency by comparing the known experimental and simulation results such as mass of silica leaving the jet mill model after fine grinding process for a wide range of operating variables.

- Simulations of the fine grinding process in air jet mill using FLUENT 6.3 solver for a wide range of operational variable changes.

- Utilization of the 3-D isometrical model of air jet mill and its 3-D and 2-D circular cross-sections at the grinding chamber region to analyze the simulation profiles such as phase distributions and velocity flow fields of air-solid phases.

- Investigation on the influence of operational variables and air-solid flow fields on the ground product characteristics such as particle size, surface pores, specific surface areas, morphologies and crystallite properties such as crystallite size, lattice strain and degree of crystallinity. Among the experimental techniques used for analysis of feed and ground product characteristics are Malvern Mastersizer, XRF, BET, SEM and XRD.

1.7 Overview of the Thesis

This thesis consists of five chapters in which Chapter One (Introduction) gave a brief introduction on fine grinding and the factors controlling the air-solid flow fields in air jet mill. This chapter also includes the problem statements which provide

basis and rationale to identify the research direction to be followed in this study. The main and measurable objectives of this study were stated clearly followed by the scope of the work and the overview of the thesis in the last section of this chapter.

Chapter Two (Literature Review) reviewed the details of past studies on air jet mill and the working principle, breakage mechanism and the features of air-solid flows in the mill. This chapter also discussed the usage of Computational Fluid Dynamics (CFD) techniques to study multiphase flows followed by the parameters controlling the fine grinding process and the air-solid flow fields in air jet mill. The important characterizations for fine grinding products such as particle size, shape and morphologies, specific surface areas, surface pore characteristics and mechanochemical effects were reviewed in detail. The final part of this chapter summarizes the particle characteristics and industrial application of silica to show the uniqueness of this study in fulfilling the requirements in this related field.

Chapter Three (Methodology) was subdivided into two parts which were the numerical and experimental studies. The numerical part discussed the modeling of air jet mill which includes identification of computational domain, geometry creation, meshing the 3-D model and specifying the boundary and continuum types. Following to this, discussions were extended into simulations of air jet mill using FLUENT 6.3 solver which include basic assumptions, governing equations, material properties, initial and boundary conditions and solution procedure. In the experimental part, detail discussions were given on the raw material, sampling and sample preparation techniques, fine grinding test works, validation approach for CFD model of air jet mill and the feed and product characterizations.

Chapter Four (Results and Discussions) which is the main body of this thesis is divided into seven main sections. The discussions in the first section were focused on the CFD modeling of air jet mill followed by numerical simulations in the second section. In the third section of this chapter, detail elaborations were given on the validations of the CFD model of air jet mill with the known experimental results such as mass of silica exiting the mill's outlet. The following section discussed the changes in the air-solid flow fields with the mill's operational parameters. Following to this, the characteristics of raw material and the ground products with changes in operating variables and air-solid flow fields were given in sections five and six of this chapter. The final section of this chapter showed the correlation between the important experimental and numerical results from air jet mill with the mill's independent variables such as grinding pressure, solid feed rate and classifier speed.

Chapter Five (Conclusions and Recommendations) contains the overall conclusions of this study. The first part of this chapter discussed the conclusions based on the main and measurable objectives of this study. In the second part of this chapter, lists of recommendations were given for future studies in this field.

CHAPTER 2

LITERATURE REVIEW

2.1 Introduction

Grinding is a unit process with a broad range of industrial applications to produce fine particles with the product size specifications for advance materials approaching the nanosize range (Cho *et al*., 2006). Recently, attention has been drawn to ultrafine grinding in the submicron range due to the development of new functional materials such as new ceramics and electronic materials in various industrial fields (Choi, 1996; Choi *et al*., 2004; Choi *et al*., 2010). Other applications are in minerals, chemicals, toners, high purity ceramics, foods, pharmaceutical powders, resin, pigments, polymer powders, plastic, cosmetic ingredients, ultrafine metal oxides, ultrafine particle for powder coating and carbon nanotubes with micron size particles exhibiting narrow size distribution, absence of contamination and ability to grind heat sensitive materials (Alfano *et al*., 1996; Benz *et al*., 1996; Tuunila and Nyström, 1998; Tasirin and Geldart, 1999; Midoux *et al*., 1999; McMillan *et al*., 2007b, Sikong *et al*., 2008; Baddour *et al*., 2009).

Grinding is divided into three stages known as coarse grinding, fine grinding and mechanical activations. In terms of size reduction aspects, it is further classified into coarse, intermediate, fine and ultrafine grindings. The fine grinding is an intermediate case between coarse grinding and mechanical activation with its aim intended for size diminishing similar to coarse grinding. Size reduction is the most

important goal in coarse grinding while the objective of mechanical activation is the changes in the structure, tension state, chemical composition and reactivity, while the fine grinding limit is determined by ductile-brittle transition state (Boldyrev *et al*., 1996; Wang and Forssberg, 2007).

The relationship between the specific energy input (kWh/t) and the product sizes is given in Figure 2.1. Generally, larger particles have a greater chance to be captured and broken if compared to smaller particles. Additionally, greater number of flaws in larger particles allows easy depletion during breakage into daughter fragments. Thus, the specific energy input (kWh/t) requirement increases as the product size declines. Collectively, all the authors (Alfano *et al*., 1996; Mebtoul *et al*., 1996; Gommeran *et al*., 2000, Fuerstenau and Abouzeid, 2002; Cui *et al*., 2006 and Wang and Forssberg, 2007) stated that 96% of energy goes to non-productive work and only about 4% is actually used to create new surfaces.

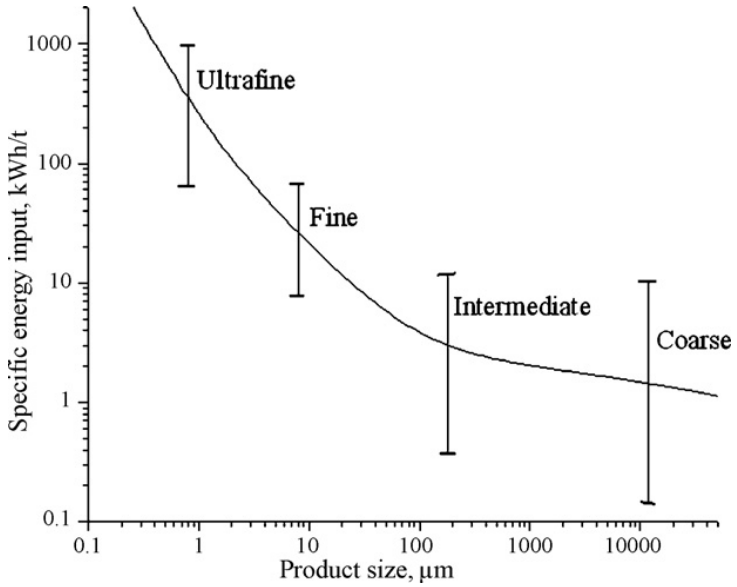

Figure 2.1: Required energy for size reduction in comminution
(Wang and Forssberg, 2007)

Grinding mills varies in their operational size range, top size of the feed material, its final achievable product sizes and the mill's specific energy inputs. The variation in specific energy input (kWh/t) with respect to mill types and its acceptable feed-product sizes are shown in Figure 2.2. Among all the mill types, stirred bead mill and fluid energy mill accept much smaller size of feed materials to produce finer products. The difference between these two mills is that the former uses beads as its grinding medium whereas the later purely operates on air as its grinding fluid.

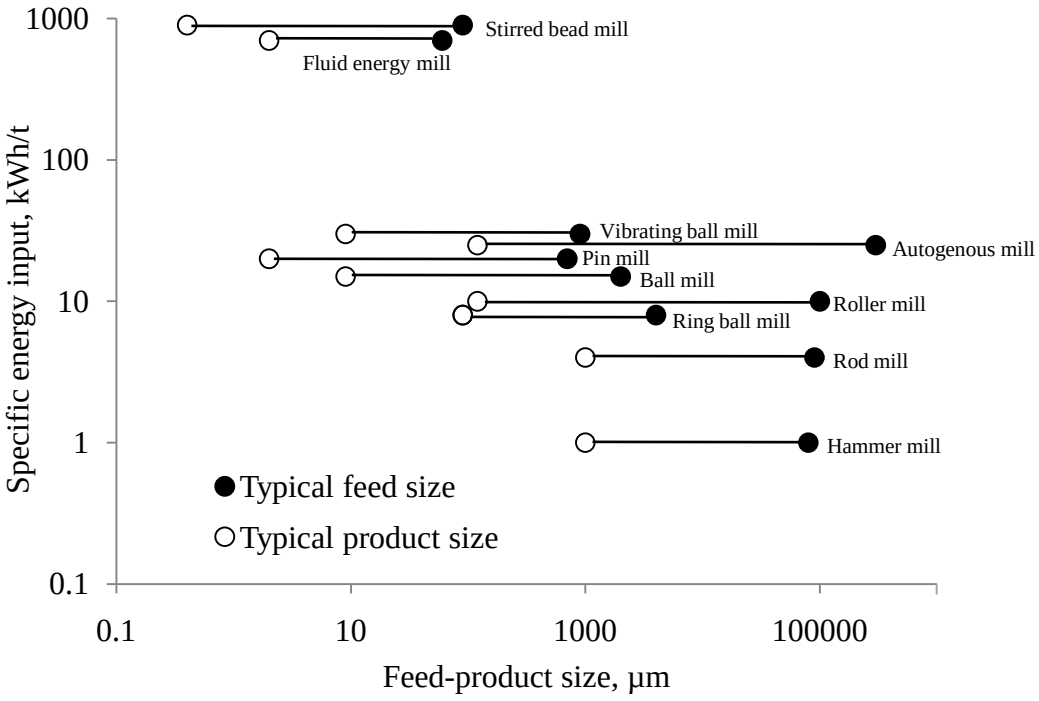

Figure 2.2: Reported average energy requirements for various mills (Wang and Forssberg, 2007)

2.2 Past Studies on Air Jet Milling

Surveying for past literatures shows that research on air jet mills are continuously progressing since it was first developed in 1960s. Various research works have been accomplished on various aspects of air jet mills. Among the pioneering studies, in 1960, Rumpf reported the acceleration of particles in a jet stream and mechanism of particle crushing using triboluminescence of sugar in a micronizer type mill. The relationships between capacity, power consumption, volumetric flow rate, solid feed rate and diameter of the air jet mills have been continuously investigated by researchers apart from its scale-up studies. Besides, in 1966, Hendry experimentally investigated a micronizer-type mill by first introducing comminution kinetics as well as classifying mechanism, while Kurten and Rumpf reported the flow pattern in a micronizer-type jet mill using water and ink as a tracer (Tanaka, 1972; Midoux *et al*., 1999).

In 1969, Ramanujam and Venkateswarlu studied the effects of jet mills design variables. The design of jet mill used in their study was different from that of the early patented mill. Later in 1982, Mohanthy and Narasimhan investigated the performance of typical air jet mill at different solid feed rates while Han *et al.* (2002, 2003) pioneered in using a model combining discrete element method (DEM) and CFD numerical method to simulate particle comminution in jet mill (Teng *et al*., 2009). Table 2.1 highlights the experimental and numerical studies on various type of air jet mills with emphasis given on the design, operating variables, material characteristics, breakage mechanism, flow behavior and product characteristics.

Table 2.1: Summary of completed works on various types of air jet mills

Researchers	Types of studies on air jet mills
Rumpf (1960)	Particles acceleration and crushing mechanism in a micronizer type mill
Hendry (1966)	Comminution kinetics and classifying mechanism in a micronizer type mill
Kurten and Rumpf (1966)	Investigation on flow pattern in micronizer type jet mill
Ramanujam and Venkateswarlu (1969)	Effects of jet mills design variables
Mohanty and Narasimhan (1982)	Performance of a typical fluid energy mill at different solid feed rates
Menyhart and Miskiewicz (1976)	Studies on the comminution and structural changes in jet mill type Fryma JMRS-80 by means of differential thermal analysis and X-ray diffractometry
Alfano *et al.* (1996)	Development of a new spiral jet mill for very fine mineral grinding
Mebtoul *et al.* (1996)	Comminution and breakage studies in spiral jet mill
Müller *et al.* (1996)	Hold up and scale up of spiral jet mills
Benz *et al.* (1996)	Performance of a fluidized bed jet mill as a function of operating variables
Tuunila and Nyström (1998)	Influence of grinding parameter of spiral jet mill towards the product fineness
Midoux *et al.* (1999)	Studies on micronization of catalyst with spiral jet mill
Tasirin and Geldart (1999)	Breakage rate in target plate and opposed nozzle jets grinding
Berthiaux *et al.* (1999)	Batch and continuous grinding kinetics studies on Alpine 100 AFG opposed air jet mill
Berthiaux and Dodds (1999)	Batch grinding kinetics and modelling fine grinding in a fluidized bed opposed jet mill
Gommeran *et al.* (2000)	Polymer grinding in spiral and opposed air jet mills and modelling the overall grinding-classification process in spiral jet mill
Frances *et al.* (2001)	Breakage mechanism of gibbsite in media mills and Alpine 100 AFG air jet mill
Godet-Morand *et al.* (2002)	Continuous grinding of talc in Alpine 100 AFG air jet mill
Han *et al.* (2002, 2003)	Combination of DEM and CFD numerical methods to simulate particle comminution in jet mill
Eskin *et al.* (1999), Eskin and Voropayev (2001a,b, 2004)	Simulation of jet milling, opposed jet milling efficiency and particulate friction in accelerating nozzles

Table 2.1 (continued)

Voropayev *et al.* (2001) Voropayev and Eskin (2002)	Simulation of interaction of opposed gas-particle jets and optimal particle acceleration in jet mill nozzles
Nakach *et al.* (2004)	Pharmaceutical powder grinding in different types of fluid jet mills
Choi *et al.* (2004)	Grinding characteristics of planetary ball mill, vibration rod mill and spiral jet mill in preparation of amorphous ultrafine particles for improvement of bioavailability of insoluble drugs
Kolacz (2004)	Grinding capacity of Comex jet mills with variation in materials and mill's operating parameters
Schlocker *et al.* (2006)	Air jet milling of solid protein-poly (acrylate) complexes for microparticle preparation
Fukunaka *et al.* (2006)	Grinding of Active Pharmaceutical Ingredients (API) with air jet mill
Levy and Kalman (2007)	Numerical study of particle motion in spiral jet mill
Katz and Kalman (2007)	Experimental analysis of spiral jet mill performance
Sikong *et al.* (2008)	Fine grinding of brittle minerals and materials using a laboratory jet mill CP-10
Ahmad *et al.* (2008)	Effect of different shapes of silica particles prepared through air jet milling in Alpine 100 AFG air jet mill on the properties of epoxy composites
Vegt de *et al.* (2006, 2009)	Influence of impurities, flaws and crystal defects of materials (salts) on Alpine 100 AFG air jet milling
Liu and Chen (2009)	Study on the flow field in the chamber of a fluidized bed opposed superfine jet mill
Teng *et al.* (2009, 2011)	Experimental and numerical analysis of a lab-scale fluid energy mill with focus on air-solid flow fields and influence of operating conditions of the vortex-type Fluid Energy Mill on the particulate motions, collisions and its relationship with particle size reduction
Palaniandy *et al.* (2008a,b,c; 2009a,b)	Effect of operating variables of Alpine 100 AFG air jet mill on fine grinding, mechanochemistry changes, product characterizations and application of products in plastic, composites, underfill encapsulant, etc.

Air jet mills use high velocity jets of gas to impart energy to particles for size reduction. These devices are commonly used in industry for fine milling of dry particulate materials. The size reduction is caused by repeated events of impacts between particles (Chamayou and Dodds, 2007; Levy and Kalman, 2007). The carrier fluid is usually compressed air but nitrogen is often used in the pharmaceutical industry for inerting purposes. Advantages of jet mills are its ability to produce micron sized particles with narrow size distribution, absence of contamination caused by autogenous grinding, low wear rate, low noise, small footprint, applicable to a wide range of material hardness, no moving parts within the chamber and their ability to grind heat sensitive materials (Berthiaux and Dodds, 1999; Midoux *et al*., 1999; Gommeran *et al*., 2000; Palaniandy *et al*., 2008a,c, 2009b).

The typical types of air jet mill are target collision type, fluidized-bed type and attrition type (Yokoyama and Inoue, 2007). The target collision type and fluidized-bed air jet mills use impact and opposed principles for size reduction while the attrition types uses spiral principle as shown in Figure 2.3 (Thaler and Roth, 2000). In the target collision type, the feed particles are accelerated by the air jet stream in the nozzle and broken by the collisions against the hard target material whereas collision between the particles is the grinding mode in a fluidized-bed air jet mill. Conversely, the attrition type has a variation in the structure with pan like shape or tubular ring like structure where the particles are mainly ground by the attrition against the particles and the tube wall. The target collision type air jet mill shows high power in grinding particles but has a drawback in terms of wear of target especially when grinding hard materials. Therefore the fluidized-bed air jet mill is

widely used for the usual fine grinding while the pan-shaped attrition type jet mill is often applied for the fine grinding of pharmaceutical materials since the cleaning is easy due to its simple structure. The principles of jet mill system are illustrated in Figure 2.3.

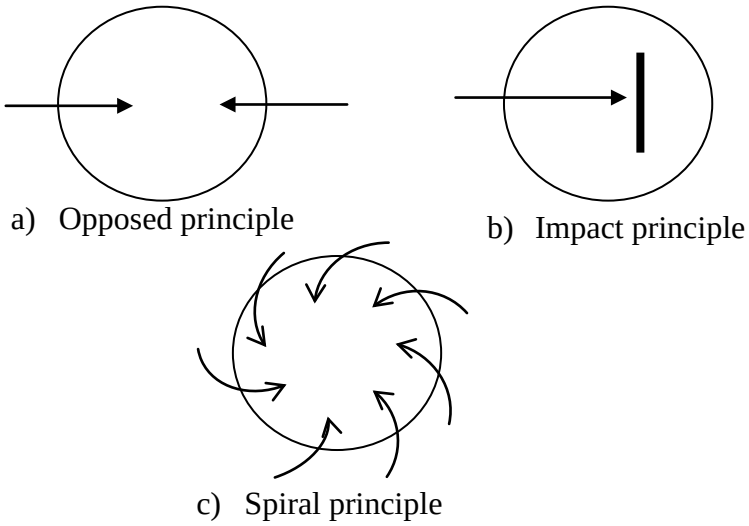

Figure 2.3: Principle of jet mill systems (Thaler and Roth, 2000)

2.2.1 Working Principle of Opposed Fluidized Bed Air Jet Mill

The cross-section of an opposed fluidized bed air jet mill which is specifically designed for continuous grinding is shown in Figure 2.4.

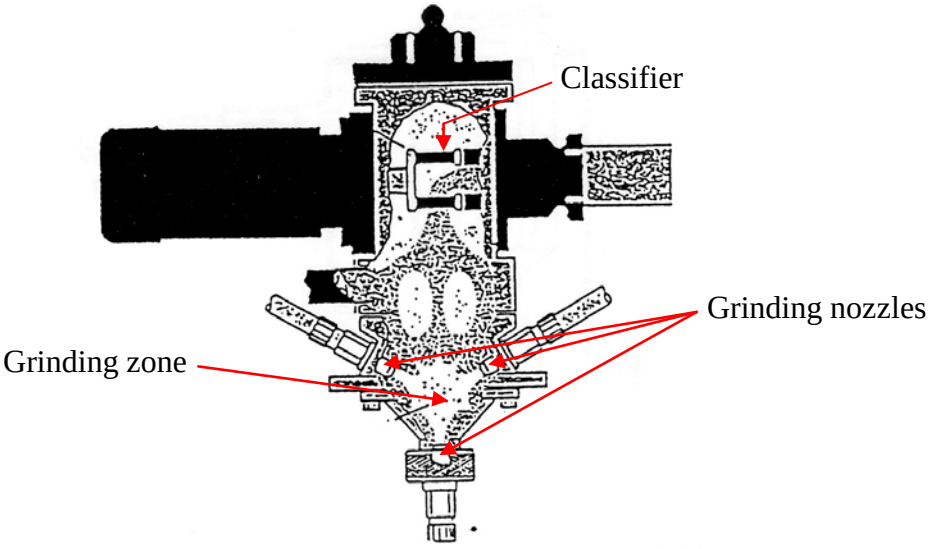

Figure 2.4: Cross-section of the grinding chamber of the Alpine 100 AFG, showing the particle flow through the mill (Berthiaux and Dodds, 1999)

The mill has a grinding chamber which is cylindrical in shape with a conical bottom. It is made of stainless steel covered with Vulkollan elastomer. The diameter of grinding chamber is 100 mm and its filling capacity is 800 cm^3. The particles to be ground enter the grinding chamber via screw feeder and are projected violently against each other by the jets of compressed air from three air nozzles of 2 mm diameter (Berthiaux and Dodds, 1999; Godet-Morand *et al*., 2002; Chan *et al*., 2002). Upon grinding, the air flow carries the ground particles to a built-in 50 mm ATP classifier which has adjustable speeds up to a maximum of 22,000 rpm (Berthiaux and Dodds, 1999).

2.2.2 Breakage Mechanism and Mode of Fragmentations in Air Jet Mill

The mode of particle fragmentations and breakage mechanism in air jet mill is dependent on the air-solid flow fields which are directly linked to the mill's design,

its operational variables and material characteristics. The typical modes of fragmentation are illustrated in Figure 2.5.

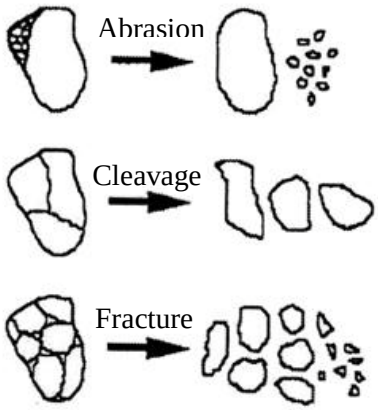

Figure 2.5: Fragmentation mechanisms (Hennart *et al*., 2009)

Abrasion results from the application of local low intensity surface stresses. It leads towards bimodal particle size distribution comprising fine particles which are released from the surface of the initial particle and particles with a size close to the size of initial particles. Conversely, cleavage of particles occurs when intense stresses are slowly applied on a particle through compression. It results in production of fragments of sizes 50 to 80 volume percent smaller than the initial particles. Apparently, fracture occurs through a rapid application of impact stresses with the particle size distribution ranges between 20 to 70 volume percent of the size of the initial particles (Varinot *et al*., 1997; Hennart *et al*., 2009). Variation in particle size distributions with fragmentation mechanisms is shown in Figure 2.6.